

Proceeding of the Korea Nuclear Society Autumn Meeting

Taejon, Korea, October 2000

An Improvement of Two-Phase, Choked Flow Model in the MARS Code

Moon-Sun Chung, Won-Jae Lee, Kwi-Seok Ha, and Sung-Jae Lee

Korea Atomic Energy Research Institute

150 Dukjin-Dong, Yusong-gu, Taejon 305-353, Korea

Abstract

A new choked flow criterion derived by the characteristic analysis of a hyperbolic two-fluid model with surface tension effect is employed in the MARS code in order to improve the two-phase, choked flow solution. The surface tension effect in the momentum equations is represented by interfacial pressure jump terms, which makes the equation system hyperbolic without any conventional source terms. Real eigenvalues are obtained for the bubbly, slug, or annular flow regime and the analytical sound speed agrees very well with the existing experimental data. Marviken critical flow tests have been assessed using the improved MARS code. The assessment results demonstrate more accurate predictions of choked flow rate for bubbly flow regime compared with the earlier choked flow solutions by Trapp-Ransom model.

1. Introduction

Choked flow condition is the inherent mathematical property of a flow model, related to eigenvalues in the governing equation system. The two-phase choking model employed in the MARS code is based on the Trapp-Ransom [1] model employed in the RELAP5/MOD3 code for non-homogeneous, non-equilibrium flow. They developed an analytic choking criterion using the characteristic analysis of the two-fluid model that includes relative phasic acceleration terms and derivative-dependent mass transfer. Comparisons to existing data indicated that the thermal equilibrium assumption was the more appropriate than the frozen flow assumption.

The two-fluid model employed in the development of two-phase choking criteria in the RELAP5/MOD3 code included an overall mass conservation, two-phase momentum equations, and the mixture energy equation written in terms of entropy. This equation set includes interface force terms called virtual mass terms due to relative acceleration. Therefore, the choking criteria are functions of homogeneous sound speed defined analytically by thermodynamic properties and virtual mass coefficient.

While the characteristic analysis included most of the time and spatial derivative terms, all of the virtual mass terms effected on the system eigenvalues [1, 2, 3]. It is significant that these eigenvalues directly participate in the choked flow criterion and its variation from the homogeneous result is entirely due to velocity non-equilibrium, since their results obtained under the assumption of thermal equilibrium.

The real part of the system eigenvalues gives the velocities of signal propagation along the corresponding characteristic path in the space/time plane and the imaginary

part gives the rate of amplitude growth of the signal propagating along the respective path. In the earlier study, analytic form of sound speed obtained by the characteristic analysis and it showed the under predicted sound speed by comparison with the experimental data in the bubbly flow regime [1]. Furthermore, the existence of the non-zero imaginary part of the system eigenvalues causes the nonphysical, short wave length instability [4, 5, 6].

A new promising approach to remove the complex eigenvalues has been proposed by the present authors: see Lee et al. [7, 8] and Chung et al. [9]. We introduced new terms about interfacial pressure force based on the surface tension terms into the momentum equations. Although these terms were relatively very small, they contributed to hyperbolicity of the equation system, without the conventional virtual mass or artificial viscosity terms and the analytically obtained eigenvalues represent comparable sound speed with the existing measured data for bubbly, slug, or annular flow. In this study, we gives a new choked flow criterion on the break flow through the initial two-phase bubbly flow regime when the fluid velocity equals or exceeds the signal propagation speed.

In this paper, we elaborated an enhancement of the choked flow model based on the earlier works of Trapp-Ransom [1] in the MARS code. It aims for a better prediction of the choked flow rate in two-phase bubbly flow. We introduce the interfacial pressure jump terms in Section 2. Following the characteristic analysis of the system matrix in Section 3, we discuss how new criterion is implemented in Section 4. Finally, in Section 5, we treat Marviken tests as the benchmark problems of two-phase choked flow.

2. Interfacial Pressure Jump Terms

Trapp-Ransom [1] had investigated the impact of the virtual mass coefficient on the sound speed. Although, the virtual mass coefficient is taken as zero, the sound speed is under predicted in the bubbly flow with void fraction range $\mathbf{a}_g < 0.5$. To preclude problems associated with the selection of C_v and the evaluation of the choking criterion, we do not include the virtual mass terms in the characteristic analysis then we can simplify the choking criterion as follows.

The conservation laws are made of one-dimensional two-fluid mass, momentum, and energy equations based on the area-averaged phasic properties.

Continuity:

$$\frac{\partial(\mathbf{a}_k \mathbf{r}_k)}{\partial t} + \frac{\partial(\mathbf{a}_k \mathbf{r}_k \mathbf{n}_k)}{\partial x} = \mathbf{f}_{c,k} \quad , \quad (1)$$

Momentum:

$$\frac{\partial(\mathbf{a}_k \mathbf{r}_k \mathbf{n}_k)}{\partial t} + \frac{\partial(\mathbf{a}_k \mathbf{r}_k \mathbf{n}_k^2)}{\partial x} + \mathbf{a}_k \frac{\partial p_k}{\partial x} + (p_k - p_i) \frac{\partial \mathbf{a}_k}{\partial x} = \mathbf{f}_{m,k} \quad , \quad (2)$$

Internal Energy:

$$\frac{\partial(\mathbf{a}_k \mathbf{r}_k u_k)}{\partial t} + \frac{\partial(\mathbf{a}_k \mathbf{r}_k v_k u_k)}{\partial x} + p_k \left[\frac{\partial \mathbf{a}_k}{\partial t} + \frac{\partial(\mathbf{a}_k v_k)}{\partial x} \right] = \mathbf{f}_{i,k} \quad , \quad (3)$$

The notation \mathbf{a}_k , \mathbf{r}_k , p_k , v_k , and u_k denote volume fraction, density, pressure, velocity, and internal energy, respectively, with phasic component $k = g$ for the gas and $k = l$ for the liquid. We will use the relation $\mathbf{a}_g + \mathbf{a}_l = 1$. The source terms $\mathbf{f}_{c,k}$, $\mathbf{f}_{m,k}$, and $\mathbf{f}_{i,k}$ depend on algebraic forms, therefore, they will not alter mathematical property of the above differential equation system.

The pressure force term on the left of momentum equation (2), $(p_k - p_i)\partial\mathbf{a}_k/\partial x$, is the term related with the surface tension as introduced by Lee et al. [7, 8] and Chung et al. [9]. Its salient feature is not that the pressure has a jump at the interface but that its gradient is continuous across the interface for bubbles in equilibrium.

The pressure discontinuity at the bubble interface due to the surface tension is taken into account in the two-phase momentum equations. Inclusion of these terms makes the equations system hyperbolic, even without conventional additive terms: See References [7, 8, 9]. The pressure force term in the left of following momentum equations is the term related to the surface tension, we got

$$(p_g - p_i)\frac{\partial\mathbf{a}_g}{\partial x} = L_g \left(1 - \frac{R_g}{2} \frac{\partial a_i}{\partial\mathbf{a}_g} \right) \frac{\partial\mathbf{a}_g}{\partial x} \quad (4)$$

$$(p_i - p_l)\frac{\partial\mathbf{a}_l}{\partial x} = -L_l \left(1 + \frac{R_l}{2} \frac{\partial a_i}{\partial\mathbf{a}_l} \right) \frac{\partial\mathbf{a}_l}{\partial x} \quad (5)$$

We use for the bubbly flow the interfacial area density relation, $a_i = 3.6\mathbf{a}_g / D_a$, suggested by Ishii and Mishima [10]. By using the definition of the mixture bulk modulus

$$L_m = -V \frac{dp}{dV} = -V \frac{dp}{dV_g + dV_l} = V \frac{dp}{V_g dp / L_g + V_l dp / L_l} \quad (6)$$

and the fluid bulk moduli $L_k \equiv \mathbf{r}_k c_k^2$, the mixture bulk modulus yields $L_m \approx \mathbf{r}_g c_g^2$ when they hold that $L_g \ll L_l$.

3. Characteristic Analysis

The eigenvalues of the equation system represent wave speed of small-amplitude short wavelength perturbations as Whitham [11] indicated. For long wavelength disturbances, dispersion and source terms play more important role while for large amplitude disturbances the nonlinear wave interaction causes dominant effect. If the eigenvalues are all real, the initial value problem is well posed and stable against small disturbances.

In a matrix form, the mass, momentum, and internal energy equations turn out

$$\frac{\partial U}{\partial t} + G \frac{\partial U}{\partial x} = A^{-1} \cdot C \quad (7)$$

where $G = A^{-1} \cdot B$ and $E = A^{-1} \cdot C$. The eigenvalues of matrix G in equation (7) are determined by a sixth-order polynomial equation:

$$P_6(\mathbf{I}) = (\mathbf{I} - v_g)(\mathbf{I} - v_l)[K_1 \mathbf{I}^4 + K_2 \mathbf{I}^3 + K_3 \mathbf{I}^2 + K_4 \mathbf{I} + K_5] = 0 \quad (8)$$

where the coefficients as functions of bulk moduli and phasic properties are

$$K_1 = 1, \quad K_2 = -2(v_g + v_l),$$

$$K_3 = \frac{1}{\mathbf{a}_l C_g^2 \mathbf{r}_g + \mathbf{a}_g C_l^2 \mathbf{r}_l} \left\{ \mathbf{a}_l C_g^2 \mathbf{r}_g \left[(v_g + v_l)^2 + 2v_g v_l - \frac{L_g}{\mathbf{r}_g} - C_l^2 \right] + \mathbf{a}_g C_l^2 \mathbf{r}_l \left[(v_g + v_l)^2 + 2v_g v_l - \frac{L_l}{\mathbf{r}_l} - C_g^2 \right] \right\},$$

$$K_4 = \frac{2}{\mathbf{a}_l C_g^2 \mathbf{r}_g + \mathbf{a}_g C_l^2 \mathbf{r}_l} \left\{ \mathbf{a}_l C_g^2 \mathbf{r}_g \left[v_g (C_l^2 - v_l^2) + v_l \left(\frac{L_g}{\mathbf{r}_g} - v_g^2 \right) \right] + \mathbf{a}_g C_l^2 \mathbf{r}_l \left[v_l (C_g^2 - v_g^2) + v_g \left(\frac{L_l}{\mathbf{r}_l} - v_l^2 \right) \right] \right\},$$

$$K_5 = \frac{1}{\mathbf{a}_l C_g^2 \mathbf{r}_g + \mathbf{a}_g C_l^2 \mathbf{r}_l} \left\{ \mathbf{a}_l C_g^2 \mathbf{r}_g \left[(C_l^2 - v_l^2) \left(\frac{L_g}{\mathbf{r}_g} - v_g^2 \right) \right] + \mathbf{a}_g C_l^2 \mathbf{r}_l \left[(C_g^2 - v_g^2) \left(\frac{L_l}{\mathbf{r}_l} - v_l^2 \right) \right] \right\}.$$

The closed-form solution to the characteristic equation (8) gives three sets of six real eigenvalues which are listed in Table 1, the three sets representing bubbly, slug, and annular two-phase flow. The first two simple eigenvalues, $I_{1,2} = v_g, v_l$, are due to contribution from the energy equations, implying that the internal energy is propagated by convection. The other two eigenvalues, I_3 and I_5 , represent approximately the sound speeds in the gas and liquid of single phase. The total sound speed of bubbly or slug flow has the void fraction weighting as

$$C_t = \frac{I_3 I_5}{a_l I_3 + a_g I_5} \quad (9)$$

For annular flow, the individual phasic sound speeds, I_3 and I_5 , are used.

The total sound speed of bubbly flow has the void fraction weighting with the closed-form solution of equation (8) as

$$C_t = \frac{C_g C_l \sqrt{\frac{r_g C_g^2}{a_l C_g^2 r_g + a_g C_l^2 r_l}}}{a_l C_g + a_g C_l \sqrt{\frac{r_g C_g^2}{a_l C_g^2 r_g + a_g C_l^2 r_l}}} \quad (10)$$

For bubbly flow, the total sound speed agrees well with the experiment [12] in the void fraction range, $0 < a_g < 0.3$, as shown in Figure 1.

Nguyen also derived the sound speed from the equations of continuity and momentum, considering a stationary wave front in a moving single-phase medium as

$$C_t = \frac{C_g C_l \sqrt{\frac{r_g r_l}{a_l C_g^2 r_g + a_g C_l^2 r_l}}}{a_g \sqrt{r_g} + a_l \sqrt{r_l}} \quad (11)$$

It is assumed that no phase change occurs during the propagation of sound wave and the

two-phase flow is confined by a rigid wall. No influence of the surface tension upon the pressure disturbance exists. Treating the interface of one phase as the elastic boundary of the other, a single-phase fluid surrounded by another fluid shows a dependency upon the bulk modulus of the other fluid, i.e. the sound speed decreases with an increasing elasticity of the other fluid.

However, Nguyen's model [13] shows nonphysical results that the sound speed is much greater than that of single-phase gas at the limiting case $\mathbf{a}_g \rightarrow 0$, as shown in Table 2. For that reason, as shown in Figure 1, some discrepancy between the present model and the Nguyen's model in the range of small void fraction $\mathbf{a}_g < 0.02$ arises. An increasing deviation shown in the void fraction range $\mathbf{a}_g > 0.3$ is possibly due to the flow regime transition effect.

4. Implementation of Choking Criterion

The two-phase choking criterion can be used as a boundary condition for obtaining flow solutions. The subroutine JCHOKER contains the choking criterion in the MARS code. The implemented choking criterion imposes on the junctions determined to be in a choked state. If choking is predicted, equation (12) is then written in terms of new-time phasic velocities and solved in conjunction with a difference momentum equation derived from the liquid and vapor momentum equations.

$$\frac{\mathbf{a}_g \mathbf{r}_l v_g + \mathbf{a}_l \mathbf{r}_g v_l}{\mathbf{a}_g \mathbf{r}_l + \mathbf{a}_l \mathbf{r}_g} = c_{he} \quad (12)$$

In the choked flow model of the MARS code, choking is assumed to occur at the

smallest section of the flow field called throat. The choking criterion can be written as a following form derived by equation (10), which is similar to the single phase choking flow criterion and choking corresponding to a total Mach number unity:

$$M_t \equiv v_t / C_t = \pm 1 \quad (13)$$

where, $v_t \equiv \frac{\mathbf{a}_g \mathbf{r}_l v_g + \mathbf{a}_l \mathbf{r}_g v_l}{\mathbf{a}_g \mathbf{r}_l + \mathbf{a}_l \mathbf{r}_g}$. In the choking test, the fluid velocity is compared to the

local sound speed, which is based on the hydrodynamic conditions at the throat. It is noted that we only apply equation (13) with (10) for the calculation of Marviken tests significantly choked in the initial bubbly flow regime.

When choking occurs, equation (13) is solved semi-implicitly with the upstream vapor and liquid momentum equations for v_g , v_l , and p_g at the point of flow choking [14]. Although the virtual mass terms have a significant effect on the wave propagation, we include only time derivative terms as momentum sources.

5. Marviken Tests

As a case of practical concern, the two-phase period of two Marviken tests 24 (L/D=0.3) and 15 (L/D=3.6) solved by including the present sound speed criterion are compared with the experiments as well as the earlier solutions by Trapp-Ransom model [1, 14]. The evolution of choking criterion for original MARS code is an improvement to choking criteria in the two-phase, bubbly flow regime taking account of equation (13).

Following discharges of mixture of subcooled and saturated water, two-phase bubbly flow period is marked by a steadily decreasing flow rate and pressure with an established vessel-water flashing rate. For that reason, the averaged discharge flow rates

of this period can be well compared with the experimental data. It is noted that we set a discharge coefficient 1.0 in the two-phase flow period for the model evaluations.

By comparisons between the calculation and the test data [15], as shown in Figure 2 and 3, the present new criterion shows better results than those given by the original choking criterion [1, 14]. The mass flow rate obtained by the Trapp-Ransom criterion is under predicted with discrepancies of 29% maximum for test 24 and represented by prolonged two-phase discharge periods for both of the test 24 and 15. Consequently, the present choking criterion improves the accuracy of predicted choked flow rates without some discharge coefficients by eliminating discrepancy between predicted sound speed and experiments.

6. Conclusion

The interfacial pressure jump term representing the surface tension effect is included in the momentum equations of two-fluid model. Total sound speeds of the two-phase mixture were obtained analytically by using the real eigenvalues of the two-fluid six-equation system. The analytical sound speeds offered good agreements with the existing measured data as well as physical enhancements of the Nguyen's model and Trapp-Ransom model at some conditions. It may be regarded as a notable advancement over the existing two-phase choked flow formulations. The new choked flow criterion has been implemented in the MARS code and assessed using Marviken critical flow tests. The comparisons of the assessment results show that the present model gives better predictions of the choked flow rate in the two-phase, bubbly flow regime.

References

1. J. A. Trapp and V. H. Ransom, Choked flow calculation criterion for nonhomogeneous, nonequilibrium two-phase flows, *Int. J. Multiphase Flow*, vol. 8, pp. 669-681, 1982.
2. D. A. Drew, L. Y. Cheng, and R. T. Lahey, Jr., The analysis of virtual mass effects in two-phase flow, *Int. J. multiphase Flow*, vol. 5, pp. 233-242, 1979.
3. A. R. D. Thorley and D. C. Wiggert, The effect of virtual mass on the basic equations for unsteady one-dimensional heterogeneous flows, *Int. J. Multiphase Flow*, vol. 12, pp. 149-160, 1985.
4. R. W. Lyczkowski et al., Characteristics and stability analyses of transient one dimensional two-phase flow equations and their finite difference approximations, *Nuclear Science and Engineering*, vol. 66, pp. 378-396, 1978.
5. J. D. Ramshaw and J. A. Trapp, Characteristics, stability, and short-wave length phenomena in two-phase flow equation systems, *Nuclear Science and Engineering*, vol. 66, pp. 93-102, 1978.
6. H. B. Stewart, Stability of two-phase flow calculation using two-fluid models, *Journal of Computational Physics*, vol. 33, pp. 259-270, 1979.
7. S. J. Lee, K. S. Chang, and K. Kim, Pressure wave speeds from the characteristics of two fluid two-phase hyperbolic equation system, *Int. J. Multiphase Flow*, vol. 24, pp. 855-866, 1998.
8. S. J. Lee, K. S. Chang, and S. J. Kim, Surface tension effect in the two-fluid equation system, *Int. J. Heat Mass Transfer*, vol. 41, pp. 2821-2826, 1998.
9. M. S. Chung, K. S. Chang, and S. J. Lee, Wave propagation in two-phase flow

based on a new hyperbolic two-fluid model, Numerical Heat Transfer, vol. 38, pp. 669-691, 2000.

10. M. Ishii and K. Mishima, Study of two-fluid model and interfacial area, NUREG/CR-1873, ANL-80-111, Argonne National Laboratory, 1980.
11. G. B. Whitham, Linear and nonlinear waves, Wiley New York, 1974.
12. R. E. Henry, M. A. Grolmes, and H. K. Fauske, Pressure pulse propagation in two-phase one- and two-component mixtures, ANL-7792, 1971.
13. K. L. Nguyen, E. R. F. Winter, and M. Greiner, Sonic velocity in two-phase systems, Int. J. Multiphase Flow, vol. 7, pp. 311-320, 1981.
14. RELAP5/MOD3.2.2 Code Manual, Volume IV: Models and Correlations, EG&G Idaho, Inc., NUREG/CR-5535, 1998.
15. The Marviken Full-Scale Critical-Flow Tests, NUREG/CR-2671, MXC-301, 1982.

Table 1. Eigenvalues in the three flow regimes

| <i>Flow Regimes</i> | <i>Eigenvalues</i> |
|---------------------|---|
| <i>Bubbly flow</i> | $I_{1,2} = v_g, v_l ; I_{3,4} = v_g \pm C_g ; I_{5,6} = v_l \pm C_l \sqrt{\frac{\mathbf{r}_g C_g^2}{\mathbf{a}_l C_g^2 \mathbf{r}_g + \mathbf{a}_g C_l^2 \mathbf{r}_l}}$ |
| <i>Slug flow</i> | $I_{1,2} = v_g, v_l ; I_{3,4} = v_g \pm C_g ; I_{5,6} = v_l \pm C_l$ |
| <i>Annular flow</i> | $I_{1,2} = v_g, v_l ; I_{3,4} = v_g \pm C_g ; I_{5,6} = v_l \pm C_l \sqrt{\frac{\mathbf{a}_l \mathbf{r}_g C_g^2}{\mathbf{a}_l C_g^2 \mathbf{r}_g + \mathbf{a}_g C_l^2 \mathbf{r}_l}}$ |

Table 2. Comparison of the effective sound speed in each phase

| <i>Flow regime</i> | <i>Present model</i> | <i>Nguyen mode</i> |
|-----------------------|---|--|
| <i>Slug flow</i> | C_l C_g | C_l C_g |
| <i>Dispersed flow</i> | $C_l \sqrt{\frac{r_g C_g^2}{a_l r_g C_g^2 + a_g r_l C_l^2}}$ C_g | $C_l \sqrt{\frac{r_g C_g^2}{a_l r_g C_g^2 + a_g r_l C_l^2}}$ $C_g \sqrt{\frac{r_l C_l^2}{a_l r_g C_g^2 + a_g r_l C_l^2}}$ |
| <i>Separated flow</i> | $C_l \sqrt{\frac{a_l r_g C_g^2}{a_l r_g C_g^2 + a_g r_l C_l^2}}$ C_g | $C_l \sqrt{\frac{a_l r_g C_g^2}{a_l r_g C_g^2 + a_g r_l C_l^2}}$ $C_g \sqrt{\frac{a_g r_l C_l^2}{a_l r_g C_g^2 + a_g r_l C_l^2}}$ |

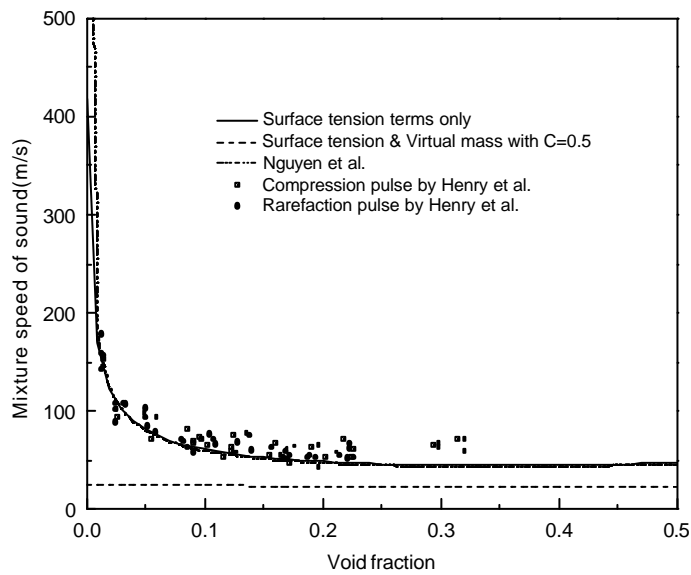


Fig. 1 Comparison of total sound speed for bubbly flow

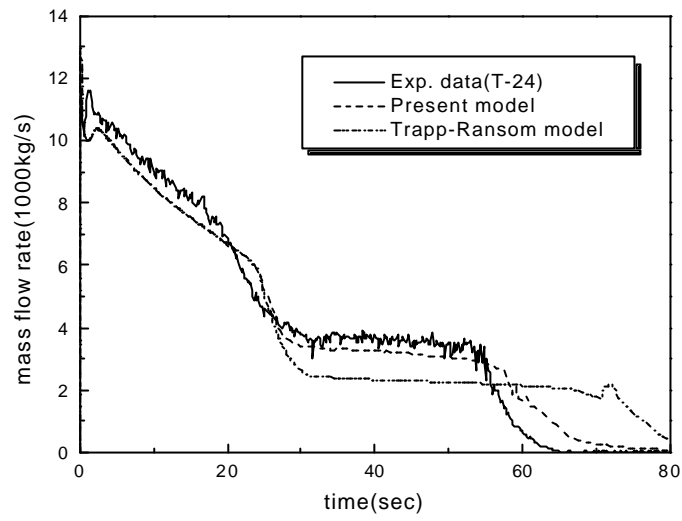


Fig. 2 Comparison between model predictions and measured data for Marviken test 24 ($L/D=0.3$)

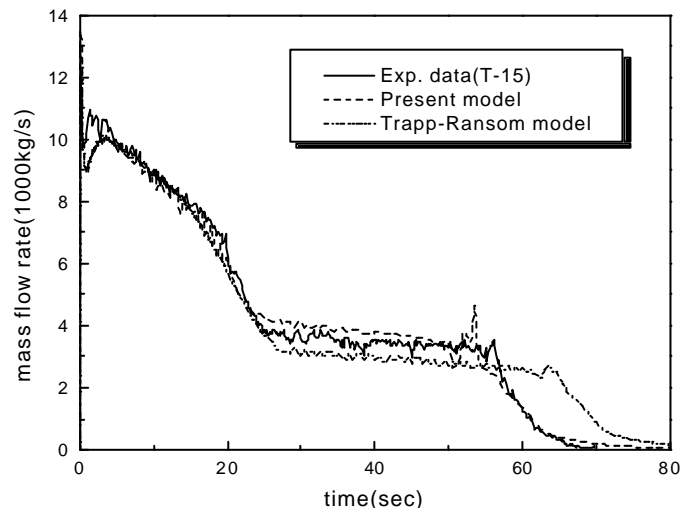


Fig. 3 Comparison between model predictions and measured data for Marviken test 15 ($L/D=3.6$)